

Microfluidic chip combined with magnetic-activated cell sorting technology for tumor antigen-independent sorting of circulating hepatocellular carcinoma cells

Xuebin Wang¹, Liying Sun^{1,2,3}, Haiming Zhang¹, Lin Wei^{1,2}, Wei Qu^{1,2}, Zhigui Zeng^{1,2}, Ying Liu^{1,2} and Zhijun Zhu^{1,2,3}

¹ Department of General Surgery, Beijing Friendship Hospital, Capital Medical University, Beijing, P. R. China

² Liver Transplantation Center, National Clinical Research Center for Digestive Diseases (NCRC-DD), Beijing Friendship Hospital, Capital Medical University, Beijing, P. R. China

³ Beijing Key Laboratory of Tolerance Induction and Organ Protection in Transplantation, Beijing Friendship Hospital, Capital Medical University, Beijing, P. R. China

ABSTRACT

Purpose: We aimed to generate a capture platform that integrates a deterministic lateral displacement (DLD) microfluidic structure with magnetic-activated cell sorting (MACS) technology for miniaturized, efficient, tumor antigen-independent circulating tumor cell (CTC) separation.

Methods: The microfluidic structure was based on the theory of DLD and was designed to remove most red blood cells and platelets. Whole Blood CD45 MicroBeads and a MACS separator were then used to remove bead-labeled white blood cells. We established HepG2 human liver cancer cells overexpressing green fluorescent protein by lentiviral transfection to simulate CTCs in blood, and these cells were then used to determine the CTC isolation efficiency of the device. The performance and clinical value of our platform were evaluated by comparison with the Abnova CytoQuest™ CR system in the separating of blood samples from 12 hepatocellular carcinoma patients undergoing liver transplantation in a clinical follow-up experiment. The isolated cells were stained and analyzed by confocal laser scanning microscopy.

Results: Using our integrated platform at the optimal flow rates for the specimen (60 $\mu\text{l}/\text{min}$) and buffer (100 $\mu\text{l}/\text{min}$ per chip), we achieved an CTC yield of $85.1\% \pm 3.2\%$. In our follow-up of metastatic patients, CTCs that underwent epithelial–mesenchymal transition were found. These CTCs were missed by the CytoQuest™ CR bulk sorting approach, whereas our platform displayed increased sensitivity to EpCAM^{low} CTCs.

Conclusions: Our platform, which integrates microfluidic and MACS technology, is an attractive method for high-efficiency CTC isolation regardless of surface epitopes.

Submitted 2 November 2018

Accepted 25 February 2019

Published 1 April 2019

Corresponding author

Zhijun Zhu,

zhu-zhijun@outlook.com

Academic editor

Shi-Cong Tao

Additional Information and
Declarations can be found on
page 14

DOI 10.7717/peerj.6681

© Copyright

2019 Wang et al.

Distributed under

Creative Commons CC-BY 4.0

OPEN ACCESS

Subjects Bioengineering, Biophysics, Drugs and Devices

Keywords Microfluidic chip, Antigen-independence, Hepatocellular carcinoma, Circulating tumor cell sorting, MACS technology

INTRODUCTION

Hepatocellular carcinoma (HCC) is one of the most common malignancies in the world (Omata *et al.*, 2017). In 1996, Mazzaferro *et al.* (1996) reported that liver transplantation (LT) was considered an optimal radical therapy for selected patients with HCC.

By removing HCC tumors with the greatest possible margin and replacing cirrhotic liver tissue with a tumor-free graft, LT has a better curative effect for liver cancer than hepatectomy (Lee *et al.*, 2010).

However, a significant proportion of HCC patients who undergo LT still suffer from unfavorable outcomes due to the chance of tumor recurrence (Trojan, Zangos & Schnitzbauer, 2016). One reason for the poor prognosis of liver cancer is that cancer cells can easily enter and spread through the bloodstream. Before surgical resection, these circulating tumor cells (CTCs) may be present in the patient's blood. Surgical operations also carry the risk of causing CTCs to enter the bloodstream (Alix-Panabières & Pantel, 2014). Thus, CTCs are currently a major focus of liver cancer research because of the key roles they play in HCC recurrence and metastasis (Masuda *et al.*, 2016; Kelley *et al.*, 2015; Choi *et al.*, 2015).

Several strategies have been used to separate blood for the analysis of CTCs. The most common enrichment approach, called immunoaffinity enrichment technology, such as applied by the CellSearch system, uses antibodies targeting epithelial cell adhesion molecule (EpCAM). This system is the only CTC isolation method currently approved by the US Food and Drug Administration for prognostic use. More recently, a number of approaches have been proposed for the isolation of CTCs using immunoaffinity selection, such as the CTC-chip (Nagrath *et al.*, 2007), GEDI (Galletti *et al.*, 2014), GEM (Sheng *et al.*, 2014), and Abnova CytoQuest™ CR (Zhao *et al.*, 2013; Hou *et al.*, 2013; Wang *et al.*, 2011), which still use EpCAM and other surface antigens as target moieties. However, CTCs may also undergo changes during disease states, such as epithelial–mesenchymal transition (EMT), accompanied by changes in CTC surface markers, leading to mesenchymal tumor cells with an increased stem-like phenotype and reduced epithelial phenotype (Giannelli *et al.*, 2016). This may be why CTC detection rates and counts achieved using this enrichment technology are generally low and the entire population of CTCs cannot be collected (De Boer *et al.*, 1999).

In this research, we attempted to combine emerging microfluidic technologies with magnetic-based cell sorting to generate a miniaturized, low-cost and antigen-independent tool for efficient CTC separation (Figs. 1A and 1B). Microfluidics, which integrates physical, chemical, and biological technologies at the microscale level, has been used to create devices known as labs-on-a-chip or micro total analysis systems. A new type of microfluidic structure using deterministic lateral displacement (DLD) was designed for the continuous high-throughput separating of whole blood from HCC patients to isolate nucleated cells, including CTCs and white blood cells (WBCs), efficiently with minimal damage and independent of antigens. Then, StraightFrom® Whole Blood CD45 MicroBeads and a magnetic-activated cell sorting (MACS) separator are used to

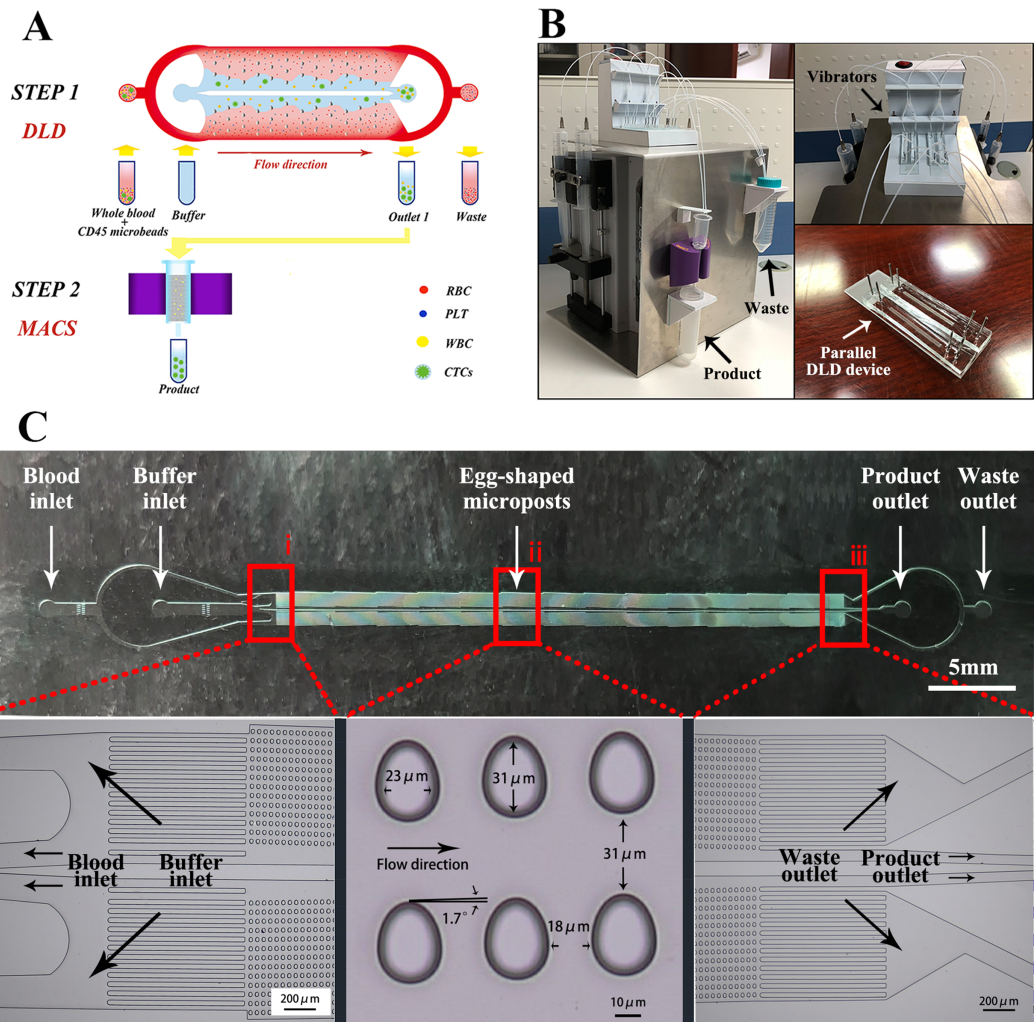


Figure 1 Platform schematic and structural design. (A) This capture platform integrates a DLD structure with a MACS separator for inline operation. Step 1: The DLD removes nucleated cells from whole blood by size-based deflection using a specially designed array of microposts. Step 2: The MACS separator serves to sensitively separate bead-labeled WBCs and unlabeled CTCs. (B) The overall system integrates syringe pumps, the DLD chip and the MACS separator into an operating platform. Before the sample enters the chip, a micro-oscillator mixes the blood to avoid stratification of the blood in the tube. (C) DLD device design. (i) Two inlets inject blood and buffer separately, the filter array ensures that blood flows along a certain direction; (ii) The device consists of two mirrored arrays of egg-shaped microposts with a pillar size and array offset designed to deflect particles larger than a certain size, thereby separating them from the main suspension; (iii) Two outlets are designed for the deflected product and undeflected waste. Photo credit: Xuebin Wang.

Full-size DOI: [10.7717/peerj.6681-fig-1](https://doi.org/10.7717/peerj.6681-fig-1)

remove bead-labeled WBCs from the DLD structure and ultimately concentrate unlabeled CTCs.

We also compared our platform with the Abnova CytoQuest™ CR system (Taipei, Taiwan) in separating and characterizing CTCs from HCC patients undergoing LT and performed follow-up analyses of HCC patients with early postoperative metastases. As CTCs from these samples underwent EMT, the detection sensitivity of the Abnova CytoQuest™ CR system was reduced, whereas our capture platform was not affected and yielded high CTC counts.

The results demonstrate that our capture platform is highly efficient independent from antigens and is thus clinically valuable.

MATERIALS AND METHODS

Deterministic lateral displacement microfluidic device design and function

The overall microfluidic DLD isolation platform is shown in Fig. 1C. This device is a size-based continuous-flow system because CTCs are generally larger in size than other blood cells (Harouaka, Nisic & Zheng, 2013). The system consists of an array of microposts with a pillar size and array offset designed to deflect particles above a certain size, thereby separating them from the main suspension (Karabacak et al., 2014). The design is based on the DLD theory proposed by Huang et al. (2004).

The flow chamber is 33 mm long, two mm wide, and 30 μm high. The microarray consists of two mirrored arrays of egg-shaped microposts, as shown in Fig. 1C, with the arrays at an angle of 1.7° with respect to the fluid flow direction. Based on the theoretical principle of DLD (Inglis et al., 2006), the critical particle diameter is approximately four to five μm . With this design, most of the red blood cells (RBCs) and platelets (PLTs) pass through the gaps and are removed through the outlet, while CTCs and some leukocytes are collected once they are concentrated.

Deterministic lateral displacement microfluidic device fabrication

Microfluidic devices were fabricated using standard photolithography and soft lithography (Faustino et al., 2016). The negative photoresist SU-8 3025 (MicroChem, Naton, MA, USA) was used to fabricate the master on a silicon wafer with a photomask. Next, polydimethylsiloxane (PDMS) prepolymer mixed with a curing agent (8:1 w/w ratio) was poured onto the silicon wafer and baked at 80 °C for 1 h; subsequently, holes were punched for the inlet and outlets. Finally, the PDMS microfluidic channels and glass substrate were exposed to oxygen plasma (PDC-M; Chengdu Mingheng Science & Technology Co., Ltd., P. R. China) for 1 min and then brought into contact to bond together. The devices were left overnight in a 65 °C oven to complete the irreversible bonding process between the PDMS and glass.

Magnetic-activated cell sorting separator and preparation

We used StraightFrom Whole Blood CD45 MicroBeads and a MACS separator (Miltenyi Biotec, Bergisch Gladbach, Germany) developed for the rapid selection of CD45⁺ cells directly from whole peripheral blood to remove bead-labeled WBCs and concentrate unlabeled CTCs. Unlike standard magnetic beads, Whole Blood CD45 MicroBeads have the advantage of not requiring sample preparation, such as density gradient centrifugation or erythrocyte lysis. MicroBeads (50 μl) were added to every one ml of anticoagulated whole blood. The samples were mixed well and incubated for 15 min in a refrigerator (2–8 °C).

Platform module integration

The overall system is shown in Fig. 1B. The platform is driven by four syringe pumps. Two of the pumps are loaded with a 50-ml syringe containing 40 ml of prepared blood

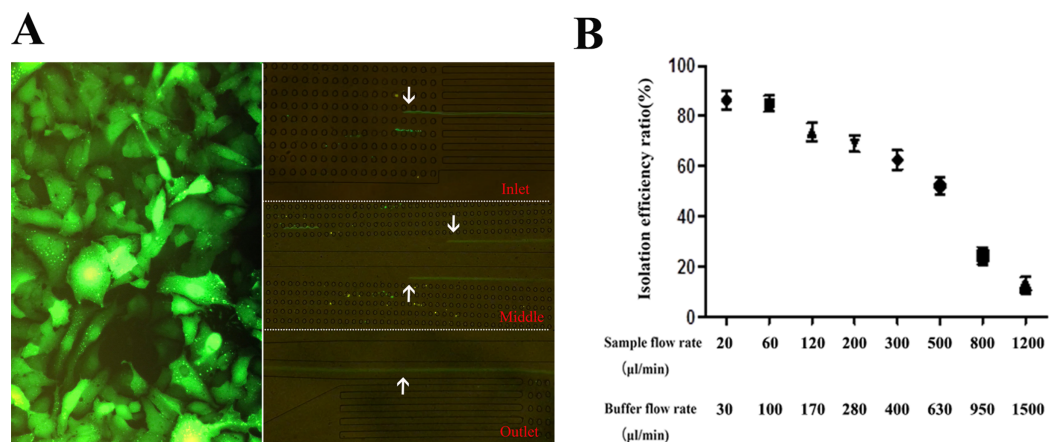


Figure 2 HepG2-GFP cells and isolation efficiency ratio with different flow rates. (A) Modeling the presence of cancer cells in human peripheral blood using HepG2-GFP cells. (B) Isolation efficiency ratio for different flow rates. A specimen flow rate of 60 µl/min and a buffer flow rate of 100 µl/min yielded an isolation efficiency ratio of $85.1 \pm 3.2\%$. [Full-size DOI: 10.7717/peerj.6681/fig-2](https://doi.org/10.7717/peerj.6681/fig-2)

suspensions, and the remaining two pumps are loaded with a 50-ml syringe containing 50 ml of phosphate-buffered saline (PBS). Teflon tubes (one mm) connect the syringe pumps to the microfluidic device, and two small vibrators are located in front of the inlets. Some leukocytes and most cancer cells are deflected to the product outlet once they are concentrated, while the remaining blood, which is diluted with buffer, is collected via waste tubing. Collected cells drop down from the product outlet of the DLD device, which contains highly bead-labeled WBCs and CTCs, and enter the MACS column. Then, magnetically labeled $CD45^+$ WBCs are retained within the column, while unlabeled cells (mostly CTCs) pass through the column and are collected at the final product outlet.

Hepatocellular carcinoma cells

To characterize the efficacy of the DLD device, we established HepG2 human liver cancer cells overexpressing green fluorescent protein (GFP) by lentiviral transfection (Fig. 2A), allowing the observation of these cells using a fluorescence microscope. Cells were cultured in low-glucose Dulbecco's modified Eagle's medium supplemented with 10% fetal bovine serum and 1% penicillin-streptomycin at 37 °C with 5% (v/v) CO_2 . The culture medium was changed every 2 days. Cells were harvested by incubation in 0.05% trypsin with 0.53 mM ethylenediaminetetraacetic acid (EDTA) at 37 °C for 3 min and were then diluted to the desired concentration.

Blood samples and follow-up

Fresh whole blood samples were collected from 10 healthy volunteers and 12 HCC patients undergoing LT (Table 1) in the Transplant Section of the Beijing Friendship Hospital in China between September 2017 and May 2018. Blood was obtained prior to transplantation for HCC patients (baseline) and then at follow-up visits 1 and 3 months after the surgery. Recurrence was diagnosed based on typical imaging findings on computed tomography (CT), magnetic resonance imaging or bone scans. At each time point, 7.5 ml of

Table 1 Patient characteristics.

Variables	Liver transplantation (<i>n</i> = 12) (%)
Sex	
Male	8(66.7)
Female	4(33.3)
Age, years	
≤50	7(58.3)
>50	5(41.7)
Etiology	
Hepatitis B	9(75)
Other	3(25)
Tumor number	
Single	5(41.7)
Multiple	7(58.3)
Tumor size, cm	
≤5	3(25)
>50	9(75)
Vascular invasion	
No	6(50)
Yes	6(50)
Milan criteria	
Within	4(33.3)
Beyond	8(66.7)

fresh whole blood was collected into EDTA-containing tubes from each subject for analysis by our DLD platform and the CytoQuest™ CR system within 6 h. Clinical information was also collected, including the alpha-fetoprotein level, size, and number of tumors, Milan criteria (Mazzaferro *et al.*, 1996), presence of hepatitis virus and vascular invasion.

Written informed consent was obtained from all patients. Approval from the Beijing Friendship Hospital Human Research Ethics Committee (code: 2018-P2-114-01) was obtained for the use of all samples using a protocol that conforms to the provisions of the Declaration of Helsinki.

Isolation efficiency of the platform integrating DLD with MACS separation

To determine the best flow rates and obtain the best isolation efficiency ratio from the device, we spiked a small number of HepG2-GFP cells into blood samples to model the presence of cancer cells in human peripheral blood. Blood samples provided by healthy volunteers were collected into EDTA-containing tubes and diluted 10 times with PBS to prevent channel blocking. HepG2-GFP cells were then spiked into the diluted blood specimens at 1×10^2 cells/ml.

The sample and buffer were injected into the specimen and buffer inlets, respectively, at different flow rates, following the principle that the sample liquid level and the buffer

liquid level would meet at the center of the chip. We counted the HepG2-GFP cells using a fluorescence microscope to select the best flow rates, and we then obtained the isolation efficiency ratio, R , using the equation $R = C_1 V_1 / (C_1 V_1 + C_2 V_2)$, where C_1 and V_1 denote the concentration and solution volume of the final product outlet, respectively, while C_2 and V_2 denote the respective concentration and solution volume of the waste outlet. The experiment was repeated 10 times.

HepG2-GFP cell sorting experiments

To examine whether there were differences in the enrichment effects of different concentrations of HCC cells, we spiked HepG2-GFP cells into 10-fold diluted whole blood at 50, 1×10^2 , 2×10^2 , 4×10^2 , and 8×10^2 cells/ml. At the best flow rates, we recalculated the isolation efficiency as described above. Each concentration was tested 10 times.

Debulking efficiency

To characterize the performance of the platform in removing blood cells (mainly RBCs, PLTs, WBCs), we spiked HepG2-GFP cells into 10-fold diluted whole blood at 1×10^2 cells/ml and injected them into the device under the best flow rates. After the device was running stably, we calculated the removal ratio R_r using the equation $R_r = (C_2 V_2 - C_1 V_1) / C_2 V_2$, where C_1 and V_1 denote the concentration and solution volume of the final product outlet, respectively, while C_2 and V_2 denote the respective concentration and solution volume of the starting sample. A hemocytometer was used to count blood cells, and the experiment was repeated 10 times.

Abnova CytoQuest™ CR system

The CytoQuest™ CR system is a rare cell sorting system developed by Abnova and the UCLA (University of California Los Angeles) Nano Research Institute. The system is a modified NanoVelcro Chip that is capable of efficiently capturing CTCs in patient blood samples using anti-EpCAM-coated silicon nanowire substrates. Circulating tumor cell enumeration by CytoQuest™ CR was carried out according to the manufacturer's protocol ([Wang et al., 2011](#); [Zhao et al., 2013](#); [Hou et al., 2013](#)). First, 7.5 ml of blood was drawn into an EDTA-containing collection tube. Next, the buffy coat containing CTCs was separated by gradient cell separation. After washing with PBS, the prepared buffy coat was injected into an EpCAM-coated microfluidic slide to capture CTCs.

Immunostaining and identification of captured cells

Circulating tumor cells were identified and counted manually. After the produced sample was transferred to a 50-ml centrifuge tube and centrifuged at $600 \times g$ for 5 min, the supernatant was aspirated. Then, the cell pellet was diluted to five ml by PBS and divided equally on 10 glass slides (Thermo Fisher Scientific, Waltham, MA, USA).

Cells on the glass slides were fixed with 4% formaldehyde for 15 min at room temperature and then permeabilized with 0.1% Triton X-100 in PBS. To identify CTCs, double immunofluorescence staining was performed with anti-cytokeratin-fluorescein isothiocyanate (anti-CK-FITC; Miltenyi Biotec, Bergisch Gladbach, Germany) and anti-CD45- allophycocyanin (anti-CD45-APC; Miltenyi Biotec, Bergisch Gladbach,

Germany). 4',6-Diamidino-2-phenylindole (DAPI; Sigma Aldrich, St. Louis, MO, USA) was used to stain nuclei. To identify CTCs undergoing EMT, cells were stained with anti-vimentin- phycoerythrin (anti-vimentin-PE; Miltenyi Biotec, Bergisch Gladbach, Germany). Cells were counted using confocal laser scanning microscopy (Lecia, Wetzlar, Germany).

The criteria for WBCs were as follows: round/ovoid, DAPI⁺/CD45⁺/CK⁻ cells $\leq 6 \mu\text{m}$ in size. Circulating tumor cells were defined as round/ovoid DAPI⁺/CD45⁻/CK⁺ cells $\geq 6 \mu\text{m}$ in size. Circulating tumor cells undergoing EMT were defined as round/ovoid, DAPI⁺/CD45⁻/CK⁺/vimentin⁺ cells $\geq 6 \mu\text{m}$ in size (Court *et al.*, 2018; Yu *et al.*, 2016).

Statistical analysis

All statistical analyses were performed using SPSS (version 22.0; IBM Corp., Armonk, NY, USA). Variance analysis was used to examine whether the isolation efficiency varied with cell concentration. A pairwise comparison between CTCs counted at different time points after detection by our integrated DLD platform and the CytoQuest™ CR system was performed by applying the nonparametric Wilcoxon signed-rank test. Graphical plots were generated using GraphPad Prism 6.0 (GraphPad Software, La Jolla, CA, USA). All *P*-values were two-sided, and *P*-values of less than 0.05 were considered statistically significant.

RESULTS

Isolation efficiency and optimal flow rates for the platform integrating DLD with MACS separation

HepG2-GFP cells were spiked into 10-fold diluted whole blood at a concentration of 1×10^2 cells/ml. At different sample flow rates of 20, 60, 120, 200, 300, 500, 800, and 1,200 $\mu\text{l}/\text{min}$, buffer was injected into the device at flow rates of 30, 100, 170, 280, 400, 630, 950, and 1,500 $\mu\text{l}/\text{min}$. The corresponding isolation efficiency ratios were $86.4\% \pm 3.7\%$ (mean \pm SD), $85.1\% \pm 3.2\%$, $73.7\% \pm 3.5\%$, $69.0\% \pm 3.3\%$, $62.5\% \pm 3.8\%$, $52.2\% \pm 3.5\%$, $24.3\% \pm 3.9\%$, and $12.6\% \pm 3.2\%$, respectively.

The cell isolation efficiency decreased significantly with increasing flow rate. To maintain a balance between isolation efficiency and time, we selected a specimen flow rate of 60 $\mu\text{l}/\text{min}$ and a buffer flow rate of 100 $\mu\text{l}/\text{min}$, which yielded an isolation efficiency ratio of approximately $85.1\% \pm 3.2\%$, as shown in Fig. 2B.

The flow of blood in the chip observed continuously through an optical microscope, as shown in Fig. 3A.

Isolation efficiency with different concentrations of cultured HCC cells

We spiked HepG2-GFP cells into 10-fold diluted whole blood at 50, 1×10^2 , 2×10^2 , 4×10^2 , and 8×10^2 cells/ml. At a specimen flow rate of 60 $\mu\text{l}/\text{min}$ and a buffer flow rate of 100 $\mu\text{l}/\text{min}$, the isolation efficiency ratio was $85.2\% \pm 3.6\%$, $85.6\% \pm 3.3\%$, $84.8\% \pm 3.3\%$, $85.0\% \pm 3.1\%$, and $85.1\% \pm 3.5\%$, respectively. Analysis of variance suggested no significant differences between the different groups ($P = 0.972 > 0.05$).

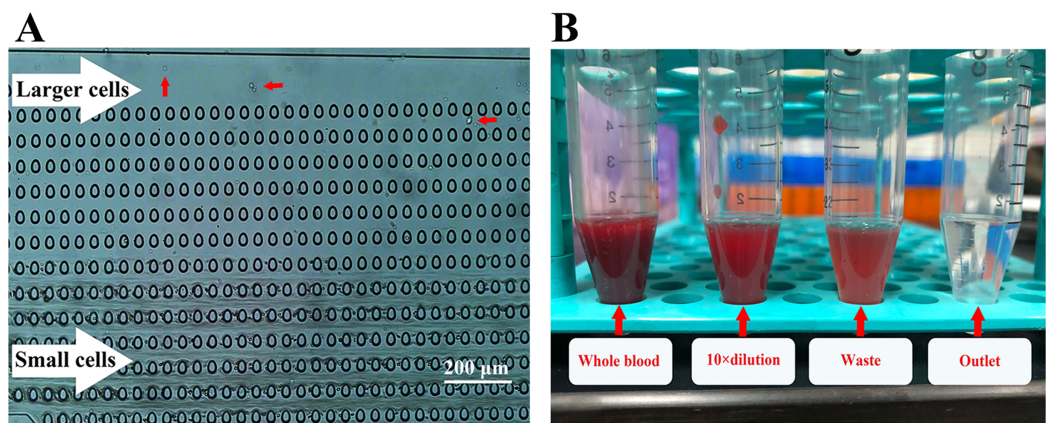


Figure 3 DLD platform enrichment experiment using blood samples. (A) The flow of blood in the chip observed through an optical microscope. Small cells, mainly composed of RBCs, flowed in a straight line, while large cells flowed at an angle and separated from the main suspension. (B) Samples obtained at different stages. Almost all RBCs were removed by the DLD chip. Photo credit: Xuebin Wang.

Full-size DOI: 10.7717/peerj.6681/fig-3

Table 2 Relative concentrations of erythrocytes, leukocytes, platelets, and HepG2-GFP recovered from the collected solution at a specimen flow rate of 60 $\mu\text{l}/\text{min}$ and a buffer flow rate of 100 $\mu\text{l}/\text{min}$.

	Concentration (%)			
	Erythrocytes	Leukocytes	Platelets	HepG2-GFP
Sample	100	100	100	100
Collected solution	0.100 ± 0.015	1.500 ± 0.017	0.050 ± 0.003	85.100 ± 3.213

Debulking efficiency and enrichment performance

The calculated results show that the RBC, WBC, and PLT removal rates were $99.90\% \pm 0.03\%$, $98.50\% \pm 0.13\%$, and $99.95\% \pm 0.05\%$, respectively. Significant changes in the appearance of the samples as shown in Fig. 3B. HepG2-GFP cells had $852 \times$ enrichment over RBCs, $57 \times$ enrichment over WBCs and $1,715 \times$ enrichment over PLTs as illustrated in Table 2.

Patient characteristics and follow-up

Among the 12 enrolled patients with HCC, 7/12 (58.3%) had multiple tumors, 9/12 (75%) had a tumor size greater than five cm, 8/12 (66.7%) extended the Milan criteria, and 6/12 (50%) had vascular invasion. Hepatocellular carcinoma recurrence after LT was observed in two patients (16.7%) during follow-up. One example of metastasis is illustrated in Fig. 4A. The patient was a 65-year-old male with diagnoses of hepatitis B cirrhosis and HCC. He underwent LT, which revealed a 20-cm dominant lesion with multiple satellite lesions and microvascular invasion. However, he was found to have multifocal lung nodules on his 3-month follow-up CT scan and then died from respiratory failure. Another example of metastasis is illustrated in Fig. 4B. The patient was a 49-year-old male with a history of hepatitis B cirrhosis and HCC who had undergone radical hepatectomy 1 year prior. Due to the recurrence of HCC, he underwent LT, which

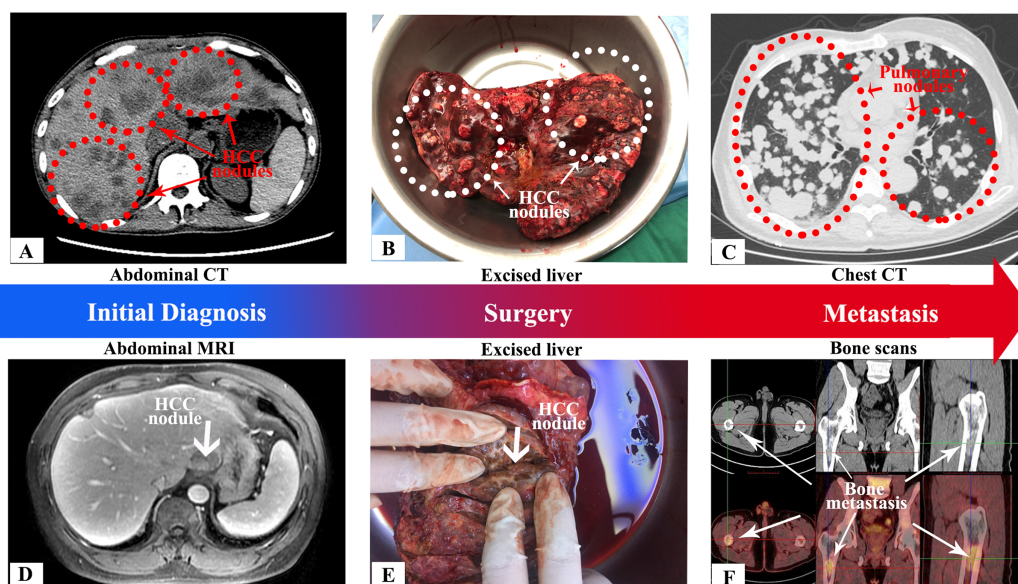


Figure 4 Preoperative CT and MRI scans, intraoperative tumor images and evidence of postoperative metastasis for two patients with tumor metastases. (A), (B), and (C) showed HCC patient no. 1. (A) Axial portal venous phase CT showed multiple, ill-defined lesions in liver (red line). The multiple lesions were presented hypodense, relative to the surrounding liver, in portal venous phase; (B) HCC nodules removed during surgery (white line); (C) Axial chest CT showed multiple, ill-defined, oval nodules in lungs (red line). The nodules were distributed at random. Combined with the clinical history, the lesions were considered as metastasis. (D), (E), and (F) showed HCC patient no. 2. (D) Axial arterial phase TIWI C⁺ showed well-defined, focal lesion in liver (arrow). The lesion was presented heterogeneous hypointense enhancement in later arterial phase; (E) HCC nodules removed during surgery (arrow); (F) Bone scans showed a focal lesion with hypermetabolism in right femoral cavity (arrow). There was no obvious bone destruction around the lesion. Based on the clinical history, the lesion was considered as metastasis. Photo credit: Xuebin Wang. [Full-size DOI: 10.7717/peerj.6681/fig-4](https://doi.org/10.7717/peerj.6681/fig-4)

revealed a three-cm dominant lesion. At 2 months after LT, bone scans indicated bone metastasis.

Ten healthy volunteers were followed for an equivalent amount of time. None of the healthy control patients involved in the study developed HCC during follow-up.

Follow-up detection of CTCs using our DLD platform and the CytoQuest™ CR system

We tested the clinical feasibility of using our device to isolate CTCs from preoperative HCC patients and healthy volunteers. We successfully collected CTCs from all HCC patients (100%), while a single CTC was found in 2/10 (20%) healthy control volunteers, representing a false positive.

The number of CTCs detected in patients by our integrated platform and the CytoQuest™ CR system is shown in [Table 3](#). Among patients with no metastasis, no significant differences in the CTC detection results were found at the three-time points by the Wilcoxon signed-rank test (preoperation: $P = 0.472 > 0.05$; 1 month postoperation: $P = 0.145 > 0.05$; 3 months postoperation: $P = 0.395 > 0.05$). However, among patients with metastasis, significantly different CTC counts were detected by our DLD platform and the CytoQuest™ CR system.

Table 3 The number of CTCs in every 7.5 ml of whole blood from patients detected by the DLD integrated platform and CytoQuest™ CR system.

No. of patients	No metastasis										Metastasis	
	1	2	3	4	5	6	7	8	9	10	1	2
Preoperation												
DLD platform CTC counts	30	11	9	12	28	14	22	26	10	36	35	25
CytoQuest™ CR CTC counts	36	9	4	13	25	16	20	25	7	38	1	5
1 month postoperation												
DLD platform CTC counts	7	4	5	9	7	3	11	10	4	10	15	10
CytoQuest™ CR CTC counts	5	1	2	6	5	5	12	13	2	8	5	6
3 months postoperation												
DLD platform CTC counts	40	5	3	11	10	7	12	9	6	5	30	20
CytoQuest™ CR CTC counts	34	5	2	9	11	4	20	9	6	4	19	15

Examination of the two metastatic patients using the CytoQuest™ CR system before and after LT revealed relatively low numbers of CTCs (preoperation: 1 and 5; 1 month postoperation: 5 and 6; 3 months postoperation: 19 and 15), whereas our DLD integrated platform collected significantly more cells (preoperation: 35 and 25; 1 month postoperation: 15 and 10; 3 months postoperation: 30 and 20).

Detection of vimentin⁺ CTCs

We further analyzed the CTCs extracted by our DLD integrated platform and the CytoQuest™ CR system before surgery by examining the expression of vimentin (Fig. 5), an EMT marker (Satelli & Li, 2011). As shown in Table 4 and Fig. 6, immunostaining showed that vimentin⁺ CTCs were found in 4/10 (40%) and 2/10 (20%) patients without metastasis by our DLD integrated platform and the CytoQuest™ CR system, respectively, and the counts were low.

DISCUSSION

Liver transplantation is used for the complete removal of tumor lesions, and the tumor recurrence and metastasis observed in HCC patients is likely related to CTCs. Therefore, the determination of CTCs by “liquid biopsies” is currently a major focus of investigation in monitoring patients with HCC undergoing LT.

In the current study, we describe a platform that integrates microfluidic DLD arrays with a MACS separator and demonstrates its great potential for tumor antigen-independent CTC separation. At the optimal specimen flow rate of 60 µl/min and buffer flow rate of 100 µl/min, a CTC isolation efficiency ratio of $85.1 \pm 3.2\%$ and a high blood cell debulking efficiency (RBC, PLT, and WBC removal rates of $99.90\% \pm 0.03\%$, $99.95\% \pm 0.05\%$, and $98.50\% \pm 0.13\%$, respectively) were achieved.

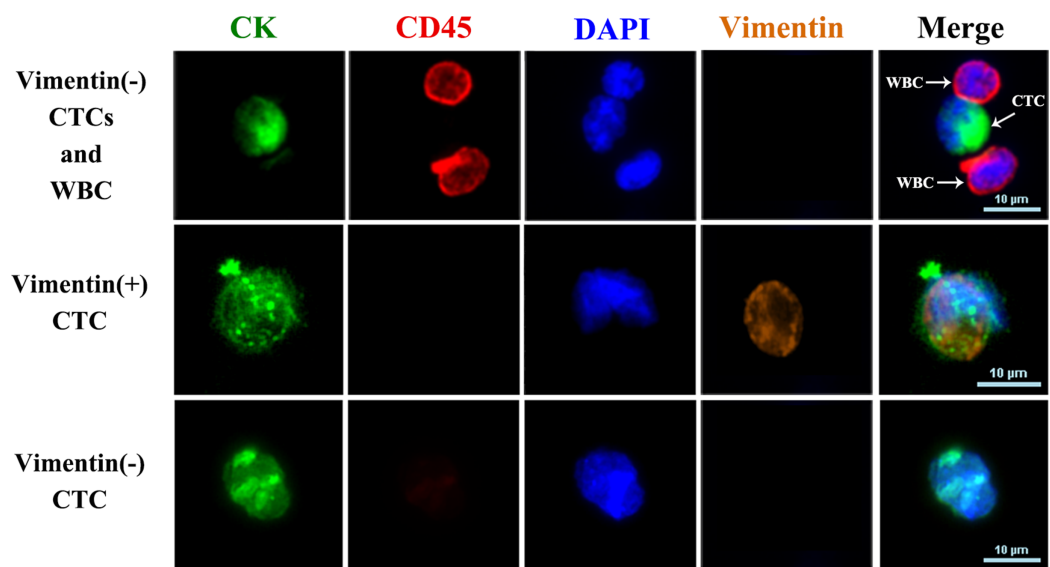


Figure 5 Fluorescence images of CTCs and WBCs. Immunofluorescence images of cells stained with antibodies against CK (green, CTC marker), CD45 (red, leukocyte marker), and DAPI (nuclear stain, blue). Anti-vimentin antibody (orange) was used to identify CTCs undergoing EMT.

Full-size DOI: 10.7717/peerj.6681/fig-5

Table 4 The number of vimentin⁻ and vimentin⁺ CTCs in every 7.5 ml of whole blood from patients before surgery detected by the DLD integrated platform and CytoQuestTM CR system.

No. of patients	No metastasis										Metastasis	
	1	2	3	4	5	6	7	8	9	10	1	2
DLD platform												
Vimentin ⁻ CTCs	27	11	9	9	28	14	20	25	10	36	7	12
Vimentin ⁺ CTCs	3	0	0	3	0	0	1	1	0	0	28	13
Total	30	11	9	12	28	14	21	26	10	36	35	25
CytoQuest TM CR system												
Vimentin ⁻ CTCs	36	9	4	12	25	16	20	25	7	36	1	3
Vimentin ⁺ CTCs	0	0	0	1	0	0	0	0	0	2	0	2
Total	36	9	4	13	25	16	20	25	7	38	1	5

In addition, there were no significant difference in the isolation performance of different tumor cell concentrations ranging from 50 to 8×10^2 cells/ml.

Furthermore, the DLD device can provide continuous CTC separation. StraightFrom Whole Blood CD45 MicroBeads have the advantage of not requiring sample preparation for the rapid selection of CD45⁺ cells directly from whole peripheral blood; thus, the cells produced from the DLD device can enter the MACS separator directly without centrifugation. Therefore, compared with other currently widely used methods for the negative selection of CTCs, such as RBC lysis or density gradient centrifugation, our capture platform has the advantage of simple operation.

At the 3-month follow-up of the 12 HCC patients undergoing LT, CTCs were found in 12 (100%) patients. Ten of the 12 patients (83.3%) did not exhibit tumor metastasis

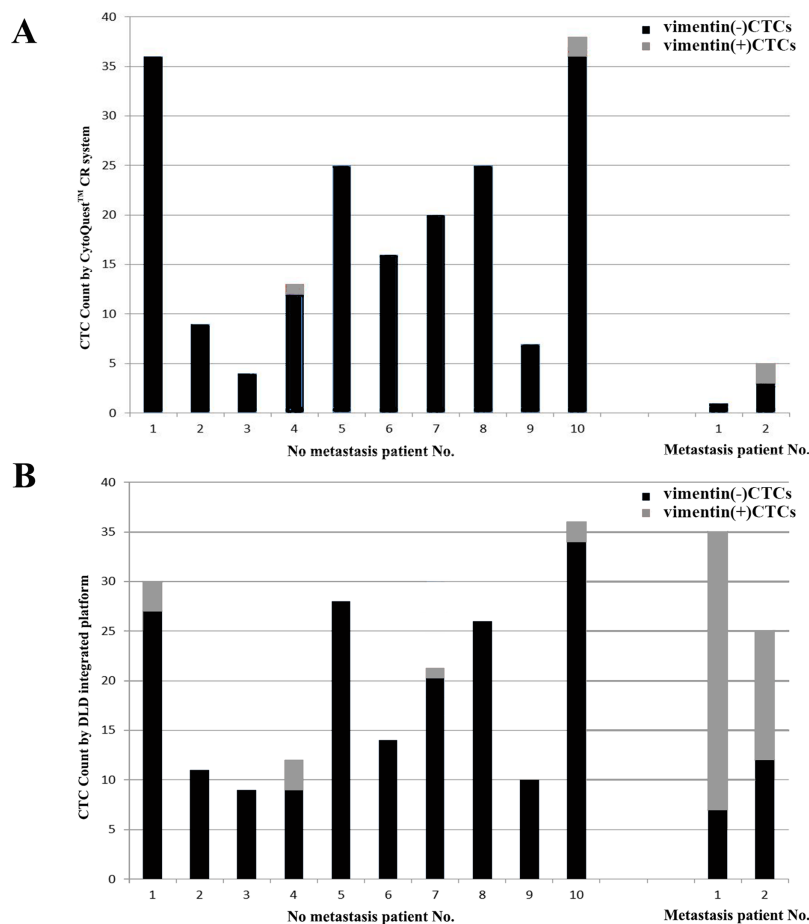


Figure 6 Numbers of CTCs that were enriched by the DLD integrated platform and CytoQuest™ CR system in HCC patients before surgery, including different subpopulations of vimentin⁺ and vimentin⁻ cells. (A) Numbers of CTCs that were enriched by CytoQuest™ CR system. (B) Numbers of CTCs that were enriched by the DLD integrated platform. [Full-size !\[\]\(f5a508cc6d05e5d06b117ced927b1acd_img.jpg\) DOI: 10.7717/peerj.6681/fig-6](https://doi.org/10.7717/peerj.6681/fig-6)

or recurrence. Two of the 12 patients (16.7%) were diagnosed with metastasis, with recurrence in the lungs ($n = 1$) and bone ($n = 1$).

Compared with the Abnova CytoQuest™ CR system, our platform yielded similar results among patients with no metastasis, as determined by the Wilcoxon signed-rank test. However, examination of the two metastatic patients using the CytoQuest™ CR system before and LT revealed relatively fewer CTCs than examination by our platform.

Our results suggest the identification of patients with tumor metastases and subpopulations of EMT-transformed CTCs. Previous studies have shown that CTCs undergo dynamic evolution under the strong selective pressure of chemotherapy, radiation therapy and any other therapeutic intervention (Aktipis *et al.*, 2011). These CTCs have lower EpCAM expression (Giannelli *et al.*, 2016) and increased metastatic potential (Mani *et al.*, 2008). Therefore, they are difficult to detect, isolate, and characterize using immunoaffinity enrichment strategies (De Boer *et al.*, 1999), and EpCAM^{low} CTCs can be missed by the CytoQuest™ CR bulk sorting approach. In contrast, our antigen-independent platform maintained a high detection sensitivity while achieving

higher CTC counts consistent with clinical observations. However, given that the sample size is relatively small, larger studies to confirm the present results are needed.

We also observed limitations of the experiments. The DLD device uses a size-based particle separation approach, but tumor cells have different diameters. Although most CTCs are larger than RBCs, there are still a small number of CTCs that are similar in diameter to RBCs (Fachin *et al.*, 2017). These cells would not be separated by the device and would eventually be lost. In addition, although CTCs were highly enriched by our platform (HepG2-GFP cells had $852 \times$ enrichment over RBCs, $57 \times$ enrichment over WBCs, and $1,715 \times$ enrichment over PLTs), the remaining cells still affect the CTC extraction purity. Finally, there is a delicate relationship between the flow rate and the separation efficiency. If researchers want to separate large volumes of blood samples at a high rate, cells under a high shear stress (Liu *et al.*, 2013) can deform because of the high fluid velocities in our device, which may influence the cell isolation efficiency.

In future studies, we will continue to improve the CTC extraction purity. In addition, using our platform, we will collect CTCs for further cell culture, drug screening, and molecular analyses.

CONCLUSIONS

Here, we demonstrate the successful use of a platform that integrates a DLD structure with a MACS separator for isolating CTC isolation with high-efficiency regardless of surface epitopes. Compared with the CytoQuest™ CR system, which is based on an immunoaffinity method, our platform successfully identified a distinct subpopulation of EMT-transformed, vimentin⁺ CTCs.

However, the device still has several limitations, as described above. Our future studies will focus on continuing to improve the device.

ACKNOWLEDGEMENTS

We thank American Journal Experts (AJE) for editing a draft of this manuscript.

ADDITIONAL INFORMATION AND DECLARATIONS

Funding

This research was supported by the China National Key Projects for Infectious Disease (No. 2017ZX100203205003004; No. 2017ZX100203205001005) and Beijing Municipal Administration of Hospitals Ascent Plan (Code: DFL20150101). The funders had no role in study design, data collection and analysis, decision to publish, or preparation of the manuscript.

Grant Disclosures

The following grant information was disclosed by the authors:

China National Key Projects for Infectious Disease: 2017ZX100203205003004 and 2017ZX100203205001005.

Beijing Municipal Administration of Hospitals Ascent Plan: DFL20150101.

Competing Interests

The authors declare that they have no competing interests.

Author Contributions

- Xuebin Wang conceived and designed the experiments, performed the experiments, analyzed the data, prepared figures and/or tables.
- Liying Sun provided blood samples.
- Haiming Zhang provided blood samples.
- Lin Wei provided blood samples.
- Wei Qu provided blood samples.
- Zhigui Zeng provided blood samples.
- Ying Liu provided blood samples.
- Zhijun Zhu contributed reagents/materials/analysis tools, authored or reviewed drafts of the paper, approved the final draft, provided blood samples.

Human Ethics

The following information was supplied relating to ethical approvals (i.e., approving body and any reference numbers):

Approval from the Beijing Friendship Hospital Human Research Ethics Committee (code: 2018-P2-114-01) was obtained for the use of all samples using a protocol that conforms to the provisions of the Declaration of Helsinki.

Data Availability

The following information was supplied regarding data availability:

The raw data are available in the figures and tables in the article.

REFERENCES

- Aktipis CA, Kwan VSY, Johnson KA, Neuberg SL, Maley CC, Jacobs DS. 2011. Overlooking evolution: a systematic analysis of cancer relapse and therapeutic resistance research. *PLOS ONE* **6(11)**:e26100 DOI [10.1371/journal.pone.0026100](https://doi.org/10.1371/journal.pone.0026100).
- Alix-Panabières C, Pantel K. 2014. Challenges in circulating tumour cell research. *Nature Reviews Cancer* **14(9)**:623–631 DOI [10.1038/nrc3820](https://doi.org/10.1038/nrc3820).
- Choi GH, Kim GI, Yoo JE, Na DC, Han DH, Roh YH, Park YN, Choi JS. 2015. Increased expression of circulating cancer stem cell markers during the perioperative period predicts early recurrence after curative resection of hepatocellular carcinoma. *Annals of Surgical Oncology* **22(S3)**:S1444–S1452 DOI [10.1245/s10434-015-4480-9](https://doi.org/10.1245/s10434-015-4480-9).
- Court CM, Hou S, Winograd P, Segel NH, Li QW, Zhu Y, Sadeghi S, Finn RS, Ganapathy E, Song M, French SW, Naini BV, Sho S, Kaldas FM, Busuttill RW, Tomlinson JS, Tseng HR, Agopian VG. 2018. A novel multimarker assay for the phenotypic profiling of circulating tumor cells in hepatocellular carcinoma. *Liver Transplantation* **24(7)**:946–960 DOI [10.1002/lt.25062](https://doi.org/10.1002/lt.25062).
- De Boer CJ, Van Krieken JH, Janssen-van Rhijn CM, Litvinov SV. 1999. Expression of Ep-CAM in normal, regenerating, metaplastic, and neoplastic liver. *Journal of Pathology* **188(2)**:201–206 DOI [10.1002/\(sici\)1096-9896\(199906\)188:2<201::aid-path339>3.0.co;2-8](https://doi.org/10.1002/(sici)1096-9896(199906)188:2<201::aid-path339>3.0.co;2-8).

- Fachin F, Spuhler P, Martel-Foley JM, Edd JF, Barber TA, Walsh J, Karabacak M, Pai V, Yu M, Smith K, Hwang H, Yang J, Shah S, Yarmush R, Sequist LV, Stott SL, Maheswaran S, Haber DA, Kapur R, Toner M. 2017. Monolithic chip for high-throughput blood cell depletion to sort rare circulating tumor cells. *Scientific Reports* 7(1):31 DOI 10.1038/s41598-017-11119-x.
- Faustino V, Catarino SO, Lima R, Minas G. 2016. Biomedical microfluidic devices by using low-cost fabrication techniques: a review. *Journal of Biomechanics* 49(11):2280–2292 DOI 10.1016/j.jbiomech.2015.11.031.
- Galletti G, Sung MS, Vahdat LT, Shah MA, Santana SM, Altavilla G, Kirby BJ, Giannakakou P. 2014. Isolation of breast cancer and gastric cancer circulating tumor cells by use of an anti HER2-based microfluidic device. *Lab on a Chip* 14(1):147–156 DOI 10.1039/C3LC51039E.
- Giannelli G, Koudelkova P, Dituri F, Mikulits W. 2016. Role of epithelial to mesenchymal transition in hepatocellular carcinoma. *Journal of Hepatology* 65(4):798–808 DOI 10.1016/j.jhep.2016.05.007.
- Harouaka RA, Nisic M, Zheng S-Y. 2013. Circulating tumor cell enrichment based on physical properties. *Journal of Laboratory Automation* 18(6):455–468 DOI 10.1177/2211068213494391.
- Hou S, Zhao H, Zhao L, Shen Q, Wei KS, Suh DY, Nakao A, Garcia MA, Song M, Lee T, Xiong B, Luo S-C, Tseng H-R, Yu H-H. 2013. Capture and stimulated release of circulating tumor cells on polymer-grafted silicon nanostructures. *Advanced Materials* 25(11):1547–1551 DOI 10.1002/adma.201203185.
- Huang LR, Cox EC, Austin RH, Sturm JC. 2004. Continuous particle separation through deterministic lateral displacement. *Science* 304(5673):987–990 DOI 10.1126/science.1094567.
- Inglis DW, Davis JA, Austin RH, Sturm JC. 2006. Critical particle size for fractionation by deterministic lateral displacement. *Lab on a Chip* 6(5):655–658 DOI 10.1039/b515371a.
- Karabacak NM, Spuhler PS, Fachin F, Lim EJ, Pai V, Ozkumur E, Martel JM, Kojic N, Smith K, Chen P-i, Yang J, Hwang H, Morgan B, Trautwein J, Barber TA, Stott SL, Maheswaran S, Kapur R, Haber DA, Toner M. 2014. Microfluidic, marker-free isolation of circulating tumor cells from blood samples. *Nature Protocols* 9(3):694–710 DOI 10.1038/nprot.2014.044.
- Kelley RK, Magbanua MJM, Butler TM, Collisson EA, Hwang J, Sidiropoulos N, Evason K, McWhirter RM, Hameed B, Wayne EM, Yao FY, Venook AP, Park JW. 2015. Circulating tumor cells in hepatocellular carcinoma: a pilot study of detection, enumeration, and next-generation sequencing in cases and controls. *BMC Cancer* 15(1):206 DOI 10.1186/s12885-015-1195-z.
- Lee KK, Kim DG, Moon IS, Lee MD, Park JH. 2010. Liver transplantation versus liver resection for the treatment of hepatocellular carcinoma. *Journal of Surgical Oncology* 101(1):47–53 DOI 10.1002/jso.21415.
- Liu Z, Huang F, Du J, Shu W, Feng H, Xu X, Chen Y. 2013. Rapid isolation of cancer cells using microfluidic deterministic lateral displacement structure. *Biomicrofluidics* 7(1):01180 DOI 10.1063/1.4774308.
- Mani SA, Guo W, Liao M-J, Eaton EN, Ayyanan A, Zhou AY, Brooks M, Reinhard F, Zhang CC, Shipitsin M, Campbell LL, Polyak K, Brisken C, Yang J, Weinberg RA. 2008. The epithelial-mesenchymal transition generates cells with properties of stem cells. *Cell* 133(4):704–715 DOI 10.1016/j.cell.2008.03.027.
- Masuda T, Hayashi N, Iguchi T, Ito S, Eguchi H, Mimori K. 2016. Clinical and biological significance of circulating tumor cells in cancer. *Molecular Oncology* 10(3):408–417 DOI 10.1016/j.molonc.2016.01.010.
- Mazzaferro V, Regalia E, Doci R, Andreola S, Pulvirenti A, Bozzetti F, Montalto F, Ammatuna M, Morabito A, Gennari L. 1996. Liver transplantation for the treatment of

small hepatocellular carcinomas in patients with cirrhosis. *New England Journal of Medicine* **334**(11):693–700 DOI [10.1056/NEJM199603143341104](https://doi.org/10.1056/NEJM199603143341104).

- Nagrath S, Sequist LV, Maheswaran S, Bell DW, Irimia D, Ulkus L, Smith MR, Kwak EL, Digumarthy S, Muzikansky A, Ryan P, Balis UJ, Tompkins RG, Haber DA, Toner M. 2007.** Isolation of rare circulating tumour cells in cancer patients by microchip technology. *Nature* **450**(7173):1235–1239 DOI [10.1038/nature06385](https://doi.org/10.1038/nature06385).
- Omata M, Cheng A-L, Kokudo N, Kudo M, Lee JM, Jia J, Tateishi R, Han KH, Chawla YK, Shiina S, Jafri W, Payawal DA, Ohki T, Ogasawara S, Chen P-J, Lesmana CRA, Lesmana LA, Gani RA, Obi S, Dokmeci AK, Sarin SK. 2017.** Asia-pacific clinical practice guidelines on the management of hepatocellular carcinoma: a 2017 update. *Hepatology International* **11**(4):317–370 DOI [10.1007/s12072-017-9799-9](https://doi.org/10.1007/s12072-017-9799-9).
- Satelli A, Li S. 2011.** Vimentin in cancer and its potential as a molecular target for cancer therapy. *Cellular and Molecular Life Sciences* **68**(18):3033–3046 DOI [10.1007/s00018-011-0735-1](https://doi.org/10.1007/s00018-011-0735-1).
- Sheng W, Ogunwobi OO, Chen T, Zhang J, George TJ, Liu C, Fan ZH. 2014.** Capture, release and culture of circulating tumor cells from pancreatic cancer patients using an enhanced mixing chip. *Lab on a Chip* **14**(1):89–98 DOI [10.1039/C3LC51017D](https://doi.org/10.1039/C3LC51017D).
- Trojan J, Zangos S, Schnitzbauer AA. 2016.** Diagnostics and treatment of hepatocellular carcinoma in 2016: standards and developments. *Visceral Medicine* **32**(2):116–120 DOI [10.1159/000445730](https://doi.org/10.1159/000445730).
- Wang S, Liu K, Liu J, Yu ZT-F, Xu X, Zhao L, Lee T, Lee EK, Reiss J, Lee Y-K, Chung LWK, Huang J, Rettig M, Seligson D, Duraiswamy KN, Shen CK-F, Tseng H-R. 2011.** Highly efficient capture of circulating tumor cells by using nanostructured silicon substrates with integrated chaotic micromixers. *Angewandte Chemie International Edition* **50**(13):3084–3088 DOI [10.1002/anie.201005853](https://doi.org/10.1002/anie.201005853).
- Yu Z, Zhang X, Zhang J, Sun B, Zheng L, Li J, Liu S, Sui G, Yin Z. 2016.** Microfluidic chip for isolation of viable circulating tumor cells of hepatocellular carcinoma for their culture and drug sensitivity assay. *Cancer Biology & Therapy* **17**(11):1177–1187 DOI [10.1080/15384047.2016.1235661](https://doi.org/10.1080/15384047.2016.1235661).
- Zhao L, Lu Y-T, Li F, Wu K, Hou S, Yu J, Shen Q, Wu D, Song M, OuYang W-H, Luo Z, Lee T, Fang X, Shao C, Xu X, Garcia MA, Chung LWK, Rettig M, Tseng H-R, Posadas EM. 2013.** High-purity prostate circulating tumor cell isolation by a polymer nanofiber-embedded microchip for whole exome sequencing. *Advanced Materials* **25**(21):2897–2902 DOI [10.1002/adma.201205237](https://doi.org/10.1002/adma.201205237).